0023-6837/00/8011-1691$03.00/0
LABORATORY INVESTIGATION
Vol. 80, No. 11, p. 1691, 2000
Printed in U.S.A.

Immunomorphometric Studies of Proteinuria in Individual Deep and Superficial Nephrons of Rats

John R. Hoyer, Agnes B. Fogo, Coleman H. Terrell, and Margaret M. Delaney

Department of Pediatrics at the Children's Hospital of Philadelphia (JRH, CHT, MMD) and University of Pennsylvania School of Medicine (JRH), Philadelphia, Pennsylvania; and Department of Pathology (ABF), Vanderbilt University School of Medicine, Nashville, Tennessee

SUMMARY: Heterogeneity of structure and function among nephrons is a well-recognized feature of chronic renal diseases. However, only a small number of superficial nephrons per kidney are accessible for micropuncture analysis and relationships of proteinuria to structural change in individual nephrons of experimental models are not clearly established. To directly evaluate proteinuria in many individual nephrons, we developed an immunomorphometric method of analysis. This method is based on the uniformly abundant renal synthesis of Tamm-Horsfall protein (THP) in the thick ascending limb of Henle's loop (TAL). Luminal rabbit immunoglobulin G (IgG) deposits are formed in TALs of proteinuric nephrons in rats injected with heterologous IgG anti-THP antibodies. This immunomorphometric luminal deposit method of assessing proteinuria was previously validated through analysis of heterologous immune complex nephropathy. Glomerular dysfunction in several models—spontaneously hypertensive rats (SHR), aging Sprague-Dawley (SD) rats, rats with adriamycin nephropathy (ADR), and rats subjected to subtotal nephrectomy (NX)—was characterized by immunomorphometric analysis after injection of anti-THP antibodies. Luminal IgG deposits were used to identify nephrons with increased proteinuria. Nephrons were identified histologically as either long looped (LL) or short looped (SL), and frequency of luminal deposits in these nephrons was determined. Glomerular size and sclerosis in deep and superficial zones of renal cortex were determined. Luminal deposits in LL nephrons were more frequent than luminal deposits in SL nephrons in SHRs ($p < .001$) and aging rats ($p < .001$) and SL nephrons in ADR rats ($p < .02$). Whole kidney levels of albuminuria correlated closely with the frequency of luminal deposits in both LL and SL nephrons of SHRs and ADR rats and in LL nephrons of aging rats ($p < .005$). In contrast, LL and SL deposits were equal in NX rats and did not correlate with albuminuria. A majority of luminal deposits extended beyond the first medullary TAL zone of NX rats, but was confined to this zone in the other 3 models. Deep cortical glomeruli were larger with more glomerulosclerosis than superficial cortical glomeruli. Albuminuria correlated with sclerosis of both deep ($p < .002$) and superficial ($p < .01$) glomeruli in NX rats, but not in the other three models. These studies provide a detailed characterization of a new method that allows comparison of proteinuria derived from deep and superficial nephrons. They also provide evidence that pathogenesis of the glomerulosclerosis in NX rats differs from that of the other three models. Glomerulosclerosis was closely linked to the overall level of albuminuria in NX rats, but not to luminal deposits. In the other three models, albuminuria and luminal deposits were closely linked but did not correlate with glomerulosclerosis. Furthermore, LL and SL nephron proteinuria of NX rats was comparable while LL proteinuria was markedly greater than SL proteinuria in the other three models. The luminal deposit method provides a new way to analyze heterogeneity of proteinuria among nephrons and the mechanisms underlying structural change in experimental glomerular diseases. (*Lab Invest 2000, 80:1691–1700*).

Proteinuria and glomerulosclerosis are well-recognized features of the renal disease of spontaneously hypertensive rats (SHRs), aging rats, rats subjected to subtotal nephrectomy (NX), and rats with adriamycin nephropathy (ADR). Although heterogeneity of structure and function among nephrons has been documented, the precise relationship of proteinuria to structural change in individual nephrons in these models has not been clearly established. Experimental evidence concerning heterogeneity of glomerular function among nephrons in several rat models has been largely derived from studies of the superficial nephrons that are accessible to micropuncture analysis (Allison et al, 1974; Fogo et al, 1988; Ichikawa et al, 1982; Lewy and Pesce, 1973; Yoshioka et al, 1988). However, analysis of deeper nephrons is only inferential, because they are not accessible for micropuncture. To provide additional information concerning heterogeneity among nephrons by directly studying proteinuria in many individual nephrons, we developed an immunomorphometric method based on the abundant renal synthesis of Tamm-Horsfall protein (THP) by the tubular cells of the thick ascending limb of Henle's loop (TAL). THP has been widely used as a marker for this tubular segment. Immunoglobulin G (IgG) anti-THP antibodies entering the ultrafiltrate of glomeruli bind to THP on the luminal surfaces of TALs (Ishidate et al, 1983), which thereby function as miniature immunoabsorbent columns for IgG anti-THP antibodies (Ishidate et al, 1992). Luminal rabbit IgG

Received June 30, 2000.
This work was supported by National Institute of Diabetes and Digestive and Kidney Diseases (NIDDK) grants RO1 DK33501 and DK44757.
Address reprint requests to: Dr. John R. Hoyer, Room 1107 Abramson Research Center, Children's Hospital of Philadelphia, 34th Street and Civic Center Blvd., Philadelphia, Pennsylvania 19104-4318. Fax: 215 590 2458; E-mail: hoyer@email.chop.edu

deposits are formed in TALs of proteinuric nephrons in rats injected with heterologous IgG anti-THP antibodies, but are not formed in the kidneys of nonproteinuric rats (Friedman et al, 1982; Ishidate et al, 1992). Thus, these luminal deposits provide a means for identifying nephrons with increased proteinuria among the many individual nephrons that can be evaluated by this method. In rats with heterologous immune complex nephropathy, a proteinuric model with a uniform pattern of glomerular hemodynamics and structural changes, the percentage of TALs with these luminal deposits is directly proportional to the overall magnitude of albuminuria (Ishidate et al, 1992). Furthermore, the distance that luminal IgG deposits extend along the course of TALs is proportional to the overall magnitude of albuminuria in this model (Ishidate et al, 1992). The renal uptake of radio-iodinated anti-THP is also proportional to the overall level of proteinuria of individual rats (Ishidate et al, 1990).

The anatomic relationships of the tubules within the outer medulla provided a basis for directly evaluating the relative contributions to overall proteinuria by long- and short-looped nephrons. TALs of long- and short-looped nephrons may be distinguished according to their proximity to vascular bundles within the inner stripe of the outer medulla. The TALs of long-looped (LL) nephrons originate from glomeruli within the deep cortex and are located at the periphery of medullary rays adjacent to vascular bundles, whereas TALs of the short-looped (SL) nephrons that originate from more superficial nephrons are separated by at least one row of tubules from vascular bundles in rat kidneys (Kriz et al, 1972: Lemley and Kriz, 1987). In these present studies, we sought to directly characterize nephrons in a new way by specifically defining the extent of proteinuria in LL and SL nephrons. This was accomplished by determining the frequency of luminal deposits within zones defined by their relative proximity to vascular bundles in the inner stripe of the outer medulla.

SHRs develop increased proteinuria and focal glomerulosclerosis that is initially restricted to the inner cortex (Feld et al, 1977). Increased protein was not detected in the glomerular filtrate of superficial glomeruli obtained by micropuncture; the proteinuria of SHRs present at the time of micropuncture was inferred to have originated from deeper glomeruli (Feld et al, 1977). Because previous studies had not reported preferential localization of glomerulosclerosis in deep glomeruli of aging Sprague-Dawley (SD) rats (Bolton et al, 1976; Couser and Stilmant, 1975; Elema and Arends, 1975), we studied aging SD rats with comparable overall levels of albuminuria as a control group. We also directly examined the relative contributions of LL and SL nephrons to proteinuria in both an ablative model and a chemically induced model by studying SD rats after subtotal nephrectomy and rats with adriamycin nephropathy. We were then able to consider, from a new perspective, the relationship of proteinuria within these nephron populations of individual rats in several experimental models of glomerular disease.

Ten male SD rats were injected intravenously with adriamycin (3 mg/kg body weight) at 8 weeks of age. At 10 weeks of age, nine male SD rats were subjected to right nephrectomy and ligation of one branch of the left renal artery to leave approximately 1/4 total kidney mass; the laterality of these procedures was reversed in an additional rat. Rats were injected with rabbit antisera to rat THP at 3 weeks after injection of adriamycin or 3 to 5 weeks after subtotal nephrectomy. Each rat received 400 μg of anti-THP antibodies/100g body weight while under light ketamine/xylazine anesthesia.

Groups of SHRs and aging rats were studied at 2 ages to achieve a relatively broad range of albuminuria in each model. A total of 15 SHRs at 11 and 14 months of age and 14 SD rats at 11 and 17 months of age were injected with rabbit anti-rat THP. Each rat received 0.6 ml/100 g of body weight of anti-THP with a maximum dose of 4.0 ml (300 μg/100 g body weight of this antisera for rats weighing $\leq$ 667 g) while under light ketamine/xylazine anesthesia.

Urine was collected from each group of rats during the 24-hour periods before and after injecting anti-THP. Renal tissue and sera were obtained at 24 hours after intravenous injection of anti-THP.

Results

General Observations

The serum levels of anti-THP antibodies of SHRs were comparable at the time of their deaths to those of aging SD rats (Table 1) and serum anti-THP levels of NX and ADR rats were comparable. Rats with a broad range of albuminuria were studied in the groups of SHRs (3.5–61 mg/24 hours) and aging SD rats (1.4–140 mg/24 hours), NX rats (2.4–50.5 mg/24 hours), and ADR rats (6.6–134.5 mg/24 hours). The mean albuminuria of SHRs, aging SD, and NX rats was comparable, and was higher in ADR rats. Serum anti-THP levels did not correlate with albuminuria in any of the models (all p values for Spearman rank coefficients > 0.4) or with the frequency of luminal deposits, glomerular hypertrophy, or sclerosis. The serum creatinine of aging SD rats had the broadest range of values (0.6–2.0 mg/dl) and was significantly associated with albuminuria ($p < .001$) and with LL ($p < .001$) and SL deposits ($p < .002$). Blood pressure measurements at weekly intervals from 30 to 36

Table 1. Albuminuria and Serum Levels

Strain	Number of rats	Albuminuria (mg/day)	Serum anti-THP (μg/ml)	Serum Creatinine (mg/dl)
SHR	15	25.1 ± 4.8	24.0 ± 1.4	0.06 ± .05
Aging	14	27.4 ± 10.0	23.8 ± 0.9	1.04 ± .10
ADR	10	70.4 ± 17.7	43.8 ± 2.4	0.70 ± .02
NX	10	23.5 ± 4.9	54.6 ± 2.5	1.15 ± .06

THP, Tamm-Horsfall protein; SHR, spontaneously hypertensive rats; ADR, adriamycin nephropathy; NX, subtotal nephrectomy.

weeks of age in representative groups of rats showed that SHRs (mean systolic pressures of 190–204 mm Hg) were persistently hypertensive relative to aging SD rats (mean systolic pressures of 125–137 mm Hg) ($p <$ .001). The times for terminal study in chronic models were based on level of albuminuria and averaged 14.0 $\pm$ 0.2 months for SHRs and 14.9 $\pm$ 0.8 months for aging SD rats. SHRs weighed less (345–430 g) than aging SD rats (512–1014 g) at these times. The initial and final weights of the NX rats were 353 $\pm$ 7 g and 339 $\pm$ 21 g, respectively. The initial and final weights of the ADR rats were 300 $\pm$ 11 g and 341 $\pm$ 17 g, respectively.

Immunofluorescence

General. The diffusely positive staining for THP allowed TALs to be readily identified (Fig. 1A). This staining was accentuated along luminal surfaces and in fine granular deposits in a distribution identical to that of basal rabbit IgG deposits. The basal deposits of THP and rabbit IgG (Friedman et al, 1982) were typically more prominent in the TALs adjacent to vascular bundles. Punctate staining for Factor $VIII_{AGN}$ was present in the endothelium of vessels in vascular bundles in the inner stripe. Because staining for Factor $VIII_{AGN}$ was confined to vascular structures, its presence did not influence the detection of rabbit IgG anti-THP deposits on luminal surfaces of TALs in triple label sections. The few tubular casts present were all strongly stained with anti-THP and only faintly stained or negative with anti-rabbit IgG. Longitudinal sections from one SHR and two aging SD rats did not contain all four TAL zones and were excluded from the analysis of the distances that luminal deposits extended along TALs.

Luminal Deposits. The rabbit IgG deposits present on the luminal surfaces of TALs (Fig. 1B) were similar in appearance to those previously described (Ishidate et al, 1983, 1992). In comparison with the strong THP staining of luminal surfaces of the same TALs, most luminal IgG deposits were smaller, less intensely stained and similar in size and intensity to basal TAL deposits (1+ deposits). The remaining luminal deposits showed greater size and intensity (2+ and 3+ luminal deposits). In general, rats with greater albuminuria had a greater percentage of TALs with luminal deposits in the inner stripe in longitudinal sections, and these deposits extended farther along TALs than in less albuminuric animals. Luminal deposits extended along TALs to similar distances in longitudinal sections from SHRs, aging SD, and ADR rats (Fig. 2). The majority of luminal deposits were confined to the inner stripe of the outer medulla in these 3 models with more luminal deposits being confined to this first TAL zone in ADR rats (68.2 $\pm$ 6.0%) than in NX rats (43.2 $\pm$ 7.7%) ($p <$ .019). Linear regression analysis showed that the overall frequency of luminal deposits in the first TAL zone of longitudinal sections correlated most closely with the albuminuria of individual ADR rats ($p <$ .001), less well with the albuminuria of aging rats ($p <$ .008) and SHRs ($p <$ .013), and not at all with the

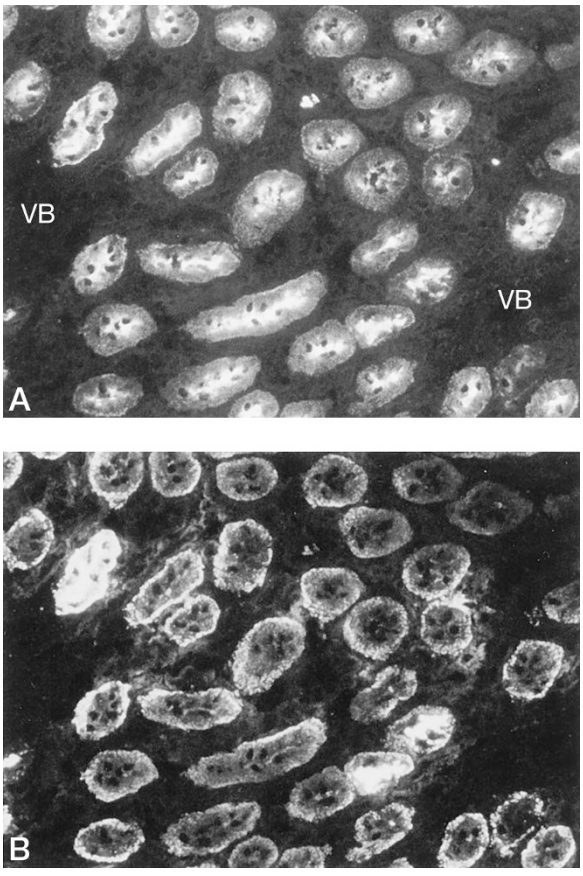

Figure 1.
Double-label immunofluorescence micrographs of a section of the inner stripe of the outer medulla in kidney from a spontaneously hypertensive rat (SHR) obtained at 24 hr after injection of rabbit anti–Tamms-Horsfall protein (THP). *A*, All thick ascending limbs of Henle's loop (TALs) show cellular staining for THP with luminal accentuation. Two vascular bundles (VB) are identified (fluorescein tagged anti-THP). *B*, Large intense luminal rabbit immunoglobulin G (IgG) deposits are present in three of the TALs adjacent to vascular bundles, whereas all TALs distant from vascular bundles show only basal granular IgG deposits (rhodamine tagged anti-rabbit IgG). Magnification: ×380.

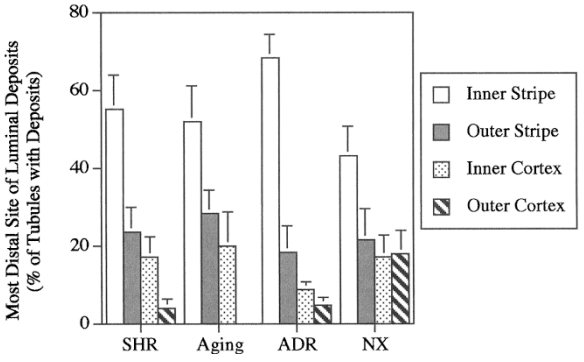

Figure 2.
Distribution of the most distal sites of luminal rabbit IgG deposits among TALs containing luminal deposits in longitudinal sections of the kidneys of SHRs (n = 14), aging Sprague-Dawley (SD) rats (n = 12), rats with adriamycin nephropathy (ADR) (n = 10), and rats subjected to subtotal nephrectomy (NX) (n = 10) at 24 hr after injection of rabbit anti-THP. The percentage of luminal deposits (mean $\pm$ SEM) in the four zones of TALs is shown. Significantly more deposits extended into the outer cortex of NX rats than in the other 3 models (see text for *p* values).

albuminuria of NX rats. Luminal deposits in some TALs extended into the inner cortex in most animals, even at low levels of albuminuria. Outer cortical luminal deposits were more frequent in NX rats (18.1 ± 6.0% of deposits) than in the three other models (all < 5% of luminal deposits), and their frequency correlated with albuminuria of individual NX rats ($p < .012$).

In sections perpendicular to the axis of medullary rays, approximately 40% of TALs were adjacent to vascular bundles (LL) (Table 2), and the distribution of TALs within the three zones of the inner stripe of the outer medulla was similar in all models. The overall percentage of TALs with luminal deposits in perpendicular sections correlated very closely with the percentage of TALs with luminal deposits in the inner stripe in longitudinal sections of individual rats in three of the four models ($p < .001$ for ADR rats, $p < .003$ for NX rats, $p < .006$ for SHRs, and $p < .06$ for aging SD rats by linear regression analysis) (Fig. 3A). Comparisons of the relative frequency of luminal rabbit IgG deposits in LL and SL nephrons in inner stripe sections showed a predominance of LL TAL deposits in SHRs and aging SD rats (Fig. 3B). LL nephrons had more deposits than SL nephrons in SHRs, aging rats, and ADR rats (Table 3), but the frequency of luminal deposits in LL and SL nephrons was comparable in NX rats. Deposits were also larger and more intense in LL nephrons than in SL nephrons of SHRs, but were comparable in LL and SL nephrons of NX rats (Fig. 3B). Luminal LL deposits were more frequent than SL deposits in all SHRs and in only half of the NX rats (Fig. 4).

In SHRs, aging SD rats, and ADR rats, the level of albuminuria was proportional to the extent of deposits in either LL or SL nephrons (Fig. 5). In contrast, albuminuria did not correlate with deposits in either LL or SL nephrons of NX rats. Albuminuria also correlated with extent of more intense deposits (≥ 2+) in LL and SL nephrons of SHRs and ADR rats and in the LL nephrons of aging SD rats (all p values < .009).

Light Microscopy

The pathological changes in each of the models were qualitatively similar to those previously described in these models and included focal thickening of glomerular and tubular basement membranes and of Bowman's capsules, as well as focal expansions of the glomerular mesangial matrix and early segmental glomerulosclerosis, focal tubular dilatation, and casts and interstitial fibrosis (Bolton et al, 1976; Couser and Stilmant, 1975; Elema and Arends, 1975; Feld et al, 1977; Fogo et al, 1988; Yoshioka et al, 1988). In general, these changes were more severe in the older rats of each group.

To define the topographic distribution of changes, the glomerular size and the extent of glomerular scle-

Table 2. Percentage of TALs Counted in Zones of Inner Stripe of Outer Medulla

Distance from vascular bundles	Long-looped nephrons		Short-looped nephrons
	Adjacent	Intermediate	Distant
SHR	38.7 ± 9.7	34.8 ± 8.1	26.5 ± 1.2
Aging	41.7 ± 1.2	31.7 ± 0.4	26.6 ± 1.3
ADR	37.6 ± 0.8	32.3 ± 0.4	30.1 ± 1.0
NX	43.8 ± 1.4	28.0 ± 0.9	28.1 ± 1.7

TALs, thick ascending limbs of Henle's loop.

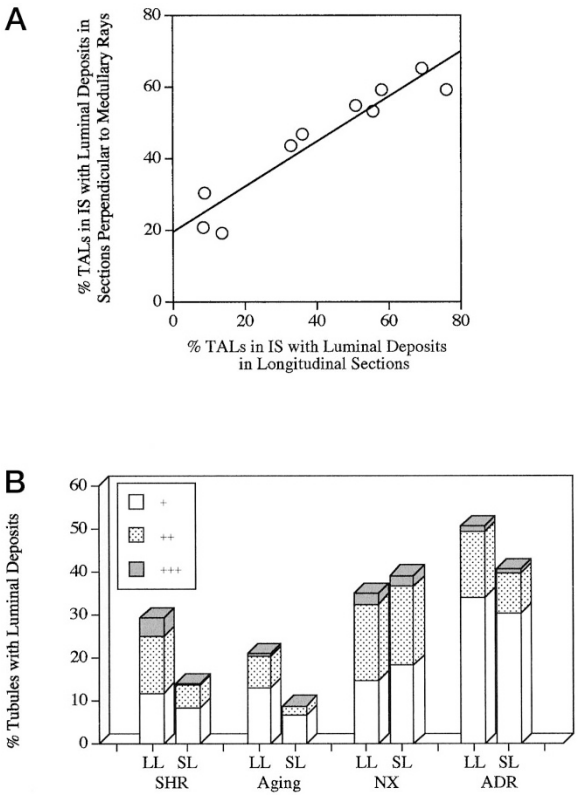

Figure 3.

A, Comparison of frequency of luminal deposits in TALs within the inner stripe of the outer medulla of ADR rats in sections perpendicular to the axis of medullary rays and longitudinal sections. The linear regression line for these ADR rats is expressed as y = .628x + 19.462, $p < .001$, $r = .948$. Regression line probabilities were $p < .003$ for NX rats, $p < .006$ for SHRs, and $p < .06$ for aging SD rats. *B*, The mean percentages of TALs with luminal rabbit IgG deposits in long-looped (LL) and short-looped (SL) nephrons are shown for SHRs (n = 15) and aging SD (n = 14), ADR (n = 10), and NX rats (n = 10). LL had more deposits than SL nephrons in SHRs and aging SD rats ($p < .001$), as well as those in ADR rats ($p < .02$). The LL deposits in SHRs were also significantly larger and more intense than in SL nephrons (≥ 2+ in 56.6 ± 4.4% vs 35.9 ± 4.2%, $p < .001$). LL nephrons of ADR rats and aging SD rats also had more ≥ 2+ luminal deposits than SL nephrons ($p < .013$ and $p < .028$ respectively). However, frequency of LL and SL deposits of NX rats was equivalent (55.5 ± 3.6% vs 58.7 ± 8.6%). (IS, inner stripe of the outer medulla.)

Table 3. Frequency of Luminal Deposits

	LL nephrons	SL nephrons	*p* value	
SHR	29.4 ± 3.5%	14.0 ± 2.0%	$p < .001$	
Aging	21.0 ± 4.5%	8.8 ± 2.3%	$p < .001$	
ADR	52.1 ± 6.3%	41.8 ± 5.8%	$p < .02$	
NX	33.0 ± 4.8%	34.3 ± 4.2%	$p > 0.5$	NS

LL, long looped; SL, short looped; NS, not significant.

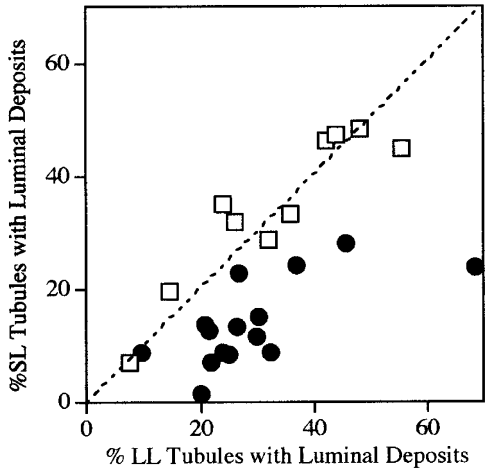

Figure 4.

Comparison of the relative frequency of luminal deposits in SL vs LL nephrons of individual SHRs (*shaded circles*) and NX rats (*open squares*). Luminal deposits in LL nephrons were more frequent than in SL nephrons in all SHRs (all points are below the broken line for equivalence), whereas half of the NX rats had more deposits in SL than LL nephrons. The regression line for SHRs is $y = .386x + 2.62$, ($p < .004$; $r = .692$) and for NX rats is $y = 0.812x + 7.54$, ($p < .001$; $r = .921$). $p < .001$ for aging SD rats and $p < .004$ for ADR rats.

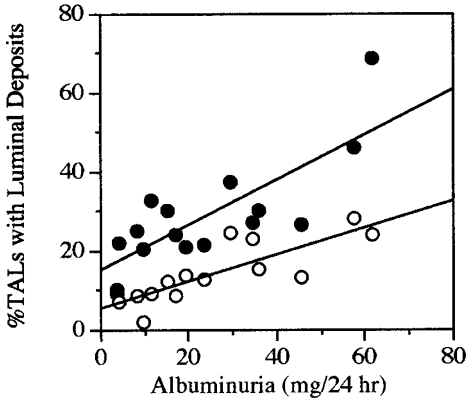

Figure 5.

Comparison of level of albuminuria of SHRs with percentages of luminal deposits in LL (*closed circles*) and SL nephrons (*open circles*). The regression line for LL nephrons is defined by $y = 14.99 + .572x$ ($p < .001$; $r = .78$) and for SL nephrons is $y = 5.47 + .338x$, ($p < .001$; $r = .83$). Regression analysis probabilities for albuminuria vs %LL deposits or %SL deposits are $p < .005$ and $p < .024$, respectively, for aging rats, and $p < .001$ and $p < .006$, respectively, for ADR rats.

rosis in the inner and outer thirds of the cortex were systematically examined. The deep glomeruli were substantially larger than the superficial glomeruli in all four models ($p < .001$) (Fig. 6, Table 4). Segmental sclerosis was present in all four models. Preferential localization of segmental sclerosis to the inner cortex was most marked in the kidneys of SHRs ($p < .001$) and ADR rats ($p < .001$) (Fig. 7, Table 4) with lesions in superficial glomeruli being quite infrequent in SHRs, aging SD rats, and ADR rats. Although superficial glomeruli of NX rats had substantial sclerosis, deep glomeruli were more severely affected in this model.

The size of deep glomeruli of individual SHRs correlated strongly with their albuminuria ($p < .002$), and

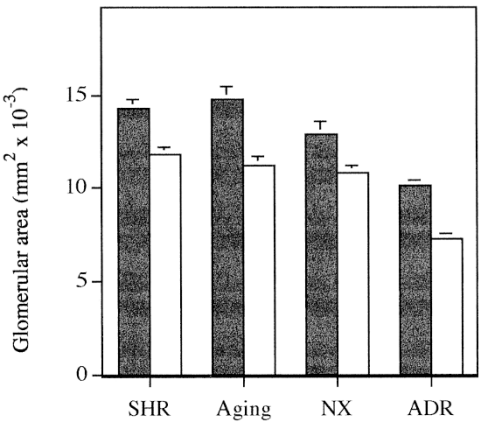

Figure 6.

Comparison of the planar areas (mean ± SEM) of deep glomeruli (*shaded bars*) vs superficial glomeruli (*open bars*) in kidneys of SHRs, aging SD rats, NX rats, and ADR rats ($p < .001$ for each model).

minimally with the frequency of intense ($\geq 2+$) luminal deposits in LL nephrons ($p < .024$). Glomerular size did not correlate with the frequency of LL deposits or with glomerulosclerosis in SHRs. Size of deep glomeruli did not correlate with albuminuria or glomerulosclerosis in ADR rats and was only weakly associated with LL deposits ($p < .016$). The size of deep glomeruli of aging SD rats did not correlate with albuminuria, glomerulosclerosis, or LL deposits.

Albuminuria of NX rats correlated with the sclerosis index of both deep ($p < .002$) and superficial ($p < .010$) glomeruli of NX rats (Fig. 8), but not with their size. The extent of glomerulosclerosis in deep and superficial glomeruli of NX rats was not significantly associated with the size of either glomerular population. The sclerosis index of deep glomeruli of NX rats was minimally associated with the frequency of $\geq 2+$ luminal deposits ($p < .042$) but not with the overall frequency of LL deposits.

Variability of glomerular size was determined as standard deviations of planar areas of deep and superficial glomeruli. The extent of size variability in the four models showed no significant correlations with their respective albuminuria, percentage of luminal deposits, or sclerosis index.

Discussion

The present studies provide direct evidence that the proteinuria of SHRs and aging SD rats is largely derived from long-looped nephrons originating in deep glomeruli. Proteinuric nephrons were identified by analysis of the distribution of the luminal IgG deposits that formed within TALs in the inner stripe of the outer medulla of rats injected with anti-TH. Because both types of TALs originate at the junction of the inner medulla and the inner stripe, many long-looped and short-looped nephrons were studied at the same distance along their TALs within this zone. The fraction of long-looped nephrons with luminal IgG deposits was more than twice as great as the fraction of short-looped nephrons with luminal deposits (Fig.

Table 4. Rat Glomeruli in Four Models of Glomerular Disease

	Planar Area[a]		Sclerosis Index		
	Deep	Superficial	Deep	Superficial	*p* value
SHR	14.3 ± 0.5	11.8 ± 0.4	0.126 ± .019	0.029 ± .009	$p < .001$
Aging	14.8 ± 0.7	11.2 ± 0.5	0.188 ± .061	0.066 ± .029	$p < .03$
ADR	10.1 ± 0.3	7.3 ± 0.3	0.149 ± .026	0.005 ± .003	$p < .001$
NX	13.0 ± 0.6	10.8 ± 0.4	0.790 ± .100	0.560 ± .150	$p < .048$

[a] All comparisons of deep vs superficial are $p < .001$.

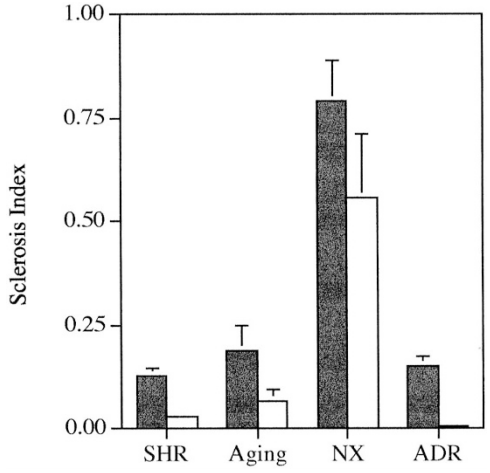

Figure 7.
Comparison of the sclerosis index (mean ± SEM) in deep (*shaded bars*) vs superficial glomeruli (*open bars*) of SHRs ($p < .001$), aging SD rats ($p < .03$), NX rats ($p < .048$), and ADR rats ($p < .001$).

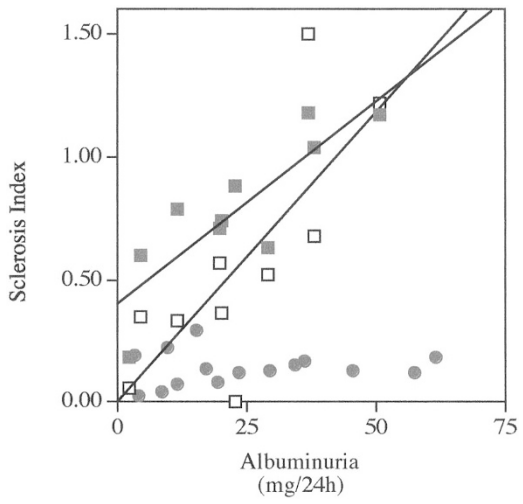

Figure 8.
Comparison of the sclerosis index of deep (*shaded squares*) and superficial glomeruli (*open squares*) of NX rats and the sclerosis index of deep glomeruli (*shaded circles*) of SHRs to their level of albuminuria. The regression lines for deep ($y = .017x + .404$; $p < .002$; $r = .847$) and superficial glomeruli ($y = .024x + .004$; $p < .010$; $r = .765$) of NX rats are shown.

3B), and more of the proteinuric long-looped nephrons were severely proteinuric. Conclusions regarding these populations of nephrons would have been more tentative if they had been based solely on studies of longitudinal sections. The concept that very proteinuric short-looped nephrons are rare in these models is supported by the scarcity of luminal deposits in the outer cortex. However, since TALs of long-looped nephrons do not extend into this zone, direct comparisons with short-looped nephrons within the outer cortex are precluded. Our results provide direct support for a previous conclusion based on indirect evidence that proteinuria originates from deep nephrons in SHRs. This conclusion was based on a lack of increased proteinuria in the filtrate of superficial glomeruli obtained by micropuncture studies of SHRs, despite overall increased proteinuria (Feld et al, 1977).

In the present study, approximately 40% of nephrons evaluated were long looped and 60% were short looped. The difference of our ratio from that of 30%:70% previously reported for the rat (Bankir and de Rouffignac, 1985) probably resulted from our selection criteria. The interbundle area was centered, with vascular bundles at the periphery of the field in the photomicrographs that were analyzed. We evaluated only those TALs whose distance from vascular bundles could be established. As expected, this method of analysis skewed the overall estimates of frequency in favor of long-looped nephrons because they are immediately adjacent to the vascular bundles. However, this allowed more precise comparisons of the populations of long- and short-looped nephrons, the goal of our studies. The populations of TALs adjacent to and distant from vascular bundles in the inner stripe were previously used in studies comparing changes in long-looped nephrons (those adjacent to vascular bundles) with changes in short-looped nephrons (Bouby et al, 1988).

Previous reports have noted that sclerosis is more severe in the deep glomeruli than in superficial glomeruli in several disease models, including the SHR rat (Feld et al, 1977). In contrast, previous studies of the glomerular lesions in aging SD rats did not report restriction of glomerulosclerosis to the deep cortex (Bolton et al, 1976; Couser and Stilmant, 1975; Elema and Arends, 1975) and glomerulosclerosis has been considered to be uniformly distributed throughout the cortex in nonhypertensive normal aging rats. Sclerosis was present in both outer cortical and inner cortical glomeruli of the aging SD rats in the current studies. However, our quantitative analysis of sclerosis and planar area in this model showed that the incidence of glomerulosclerosis is much greater in the larger deep glomeruli (Figs. 6 and 7). Greater proteinuria within

long-looped nephrons was evident at all levels of albuminuria in aging SD rats and in SHRs (Figs. 4 and 5). Taken together, these studies of SHRs and aging SD rats indicate that glomerular hypertrophy, sclerosis, and permeability to proteins are all much greater in LL nephrons than SL nephrons in both models. Markedly greater glomerular hypertrophy and sclerosis of LL nephrons were also features of the ADR model, although differences in the protein permeability of LL nephrons and SL nephrons were minimal.

Analysis of correlations between heterogeneously distributed lesions in individual rats in the present studies discloses relationships that may be pertinent to their pathogenesis. The present studies confirm the close linkage between albuminuria and the percentage of TALs with luminal deposits as well as the distance that these deposits extend in heterologous immune complex nephropathy (Ishidate et al, 1992). The percentage of LL or SL nephrons with luminal deposits in SHRs, aging SD rats, and ADR rats correlated very closely with the level of albuminuria of individual rats in each model. The percentage of LL nephrons with large and intense luminal deposits also correlated closely with albuminuria in each of these 3 models. In striking contrast to findings in the other models, luminal deposits were not selectively localized in the LL nephrons with larger glomeruli in NX rats. Furthermore, frequency of their luminal deposits did not correlate with albuminuria. These findings in NX rats indicate that proteinuria and glomerular hypertrophy are not invariably linked to each other. In contrast to findings in the other three models, the level of albuminuria correlated with sclerosis in both deep and superficial glomeruli of individual NX rats. The NX model was also the only model in which albuminuria was not tightly linked to the frequency of luminal deposits in either LL or SL nephrons.

The greater incidence of glomerulosclerosis in the deep nephrons in SHRs, aging SD rats, and ADR rats was not clearly linked to increases in either albuminuria or to the frequency of luminal deposits in LL nephrons of individual rats. Thus, these studies suggest that although albuminuria and glomerular hypertrophy are closely linked in SHRs, we did not find evidence that proteinuria is directly linked to the development of glomerulosclerosis in these three experimental models. It is important to consider potential explanations for nonconcordance of sclerosis with other features in these models. It should be noted that present observations support and extend our previous direct analysis of superficial glomeruli in the NX model in rats that indicated that proteinuria is primarily derived from "intact" nephrons that are not yet undergoing sclerosis (Yoshioka et al, 1988). Moreover, advanced sclerosis is associated with a decrease in filtration and thereby tends to reduce the proteinuria that would be otherwise derived from the glomeruli that have sustained the most severe injury. Additional recent studies have also noted a dissociation of proteinuria and glomerulosclerosis. For example, prevention of early phase proteinuria did not affect subsequent glomerulosclerosis in puromycin aminonucleoside nephropathy, and conversely therapy that prevented progressive glomerulosclerosis did not affect this early proteinuria (Tanaka et al, 1994).

Proteinuria has been proposed to be injurious, based on observations that glomerular disease accompanied by severe proteinuria often has a worse prognosis than glomerular disease with less proteinuria. Indeed, in a recent study, urinary protein excretion rate was the best independent predictor of end stage renal failure in nondiabetic chronic nephropathies (Ruggenenti et al, 1998). However, in a large study of hypertensive patients with secondary segmental glomerulosclerosis, no difference in prognosis was seen in patients with marked proteinuria versus those with lesser levels (Wehrmann and Bohle, 1998). Whether proteinuria is merely a marker of injury or a contributor to progressive injury continues to be debated (Oikawa and Fogo, 1995). Both the absence of progressive scarring in patients, even with long-standing, relapsing, minimal-change disease, and also the slowly progressive scarring that occurs in only a subset of patients with membranous glomerulonephritis, suggest that proteinuria in and of itself may not be sufficient to cause scarring. Rather, it is possible that interactions with other injurious mechanisms are necessary for sclerosis to develop. The molecular mechanisms that determine whether injury results in profound proteinuria alone, or progressive matrix accumulation, have not been elucidated. Proteinuria induced by the injection of exogenous albumin is tightly linked to the development of tubulointerstitial scarring (Eddy, 1994). Filtered neutral lipid in proteinuric states may have additional pathogenic effects on matrix accumulation (Kees-Folt et al, 1994). Divergence of glomerulosclerosis and proteinuria is also illustrated by experiments in analbuminemic rats. These rats develop the same degree of glomerular sclerosis and renal failure in response to adriamycin as do normal Sprague-Dawley rats, despite having 70% less proteinuria (Okuda et al, 1992).

Structural changes ultimately leading to end-stage, small scarred glomeruli are the consequence of the interactions of a variety of factors, which likely converge on a common process of excess matrix production. Growth factors have emerged as central modulators of this enhanced matrix production (Fogo and Ichikawa, 1989). Glomerular hypertrophy may be an indicator of such enhanced stimuli that influence both cell growth and matrix production. The present studies extend previous evidence that deep nephrons show greater glomerular hypertrophy and are more susceptible to progressive changes. However, they also demonstrate dissociation of sclerosis of hypertrophied inner cortical glomeruli from the proteinuria that originates from these nephrons.

Materials and Methods

Male spontaneous hypertensive rats, SHR/NHsdBR (SHR), 3 months old, or 7- to 9-month-old SHR retired breeders, obtained from Harlan Sprague Dawley, Inc. (Indianapolis, Indiana), and male Sprague-Dawley (SD) CD rats, 7 to 9 weeks old, and 7- to 9-month-old

retired breeders, obtained from Charles River Breeding Labs (Wilmington, Massachusetts), were fed standard rat chow containing 23% protein. Timed urine collections were periodically obtained in metabolic cages. These collections were taken the day before renal ablation or injection of adriamycin, at weekly intervals thereafter, and during the periods 24 hours before and after injection with anti-THP. Urinary excretion of rat albumin was determined by single radial immunodiffusion using agarose plates with monospecific rabbit antisera to rat albumin, as previously described (Ishidate et al, 1983). Urinary albumin excretion of all NX rats (0.31 ± .05 mg/24 hr) and ADR rats (0.35 ± .04 mg/24 hr) was normal before their initial procedures.

Blood pressure was measured in conditioned awake rats by the tail cuff method, using a tail cuff and pulse transducer (Narco Scientific, Houston, Texas) connected to a Grass polygraph (Grass Medical Instruments, Quincy, Massachusetts). During each session, at least three readings in a quiescent state were obtained from each rat. Representative groups of eight SHRs and five SD rats were examined at weekly intervals from 30 to 36 weeks of age and at death to determine blood pressure levels.

Rabbit antisera to rat THP was prepared as previously described (Hoyer et al, 1974). The antiserum used for injection contained 500 μg/ml of anti-THP antibodies and was titered as previously described using affinity-purified antibodies as original standards (Ishidate et al, 1990). Serum anti-THP levels were determined by ELISA as previously described (Ishidate et al, 1990) using 96 well flat-bottomed polystyrene microtiter plates (Nunc, Roskilde, Denmark). Dilutions of the rabbit antiserum to rat THP used for injection were included as standards on each plate.

Blocks of tissue for immunofluorescence studies were snap frozen in isopentane that was prechilled in liquid nitrogen and then were stored at −70° C until sectioned in a Slee cryostat at 4 μm. Sections were stained with fluorescein (FITC) tagged anti-rat THP (Hoyer et al, 1974) to identify TALs, and anti-Factor $VIII_{AGN}$ (Hoyer et al, 1978), an endothelial marker that does not stain tubules, to identify vascular bundles. Sections were also stained with anti-rat GBM (Hoyer et al, 1978), to identify glomeruli, and anti-proximal tubular fraction 1A (Fx1A), to identify proximal tubules (Ishidate et al, 1992) as previously described, and with rhodamine conjugated goat anti-rabbit IgG (Rho-GARG) (Cappel-Cooper Biomedical, Malvern, Pennsylvania), to detect anti-THP deposits. For double-label studies, sections were sequentially incubated with Rho-GARG, then with normal rabbit serum, to block unreacted anti-rabbit IgG sites, and then FITC tagged rabbit antibodies as previously described (Hoyer, 1980). For triple-label studies, sections were incubated with rabbit anti-Factor $VIII_{AGN}$ before double-label staining using Rho-GARG and FITC-anti-THP.

Quantitation of Luminal Deposits

Longitudinal sections of renal tissue (parallel to the axis of medullary rays in the inner stripe of the outer medulla) extending from the inner medulla to the renal capsule were studied by immunofluorescence. The distance that deposits extended along TALs within four zones was determined as previously described (Ishidate et al, 1992). The boundaries of the inner stripe (IS) and outer stripe (OS) of the outer medulla, and the inner cortex (IC) and outer cortex (OC), were defined on the basis of the tubular populations identified by immunofluorescence as previously described (Ishidate et al, 1992). The number of THP-positive tubules with luminal rabbit IgG deposits was determined by double-label immunofluorescence in consecutive fields in the middle portion of each zone. All fields in two to three frozen sections per rat were evaluated. The most distal sites of luminal deposits were determined by calculating the percentage of tubules with luminal deposits that did not extend beyond that zone as previously described (Ishidate et al, 1992).

Sections of the inner stripe of the outer medulla perpendicular to the axis of medullary rays were used for the analysis of luminal deposits in TALs in this zone. These sections were verified to be deeper than the outer stripe by the absence of proximal tubular Fx1A staining. These cross sections allow the proximity of TALs to vascular bundles to be defined. Color photomicrographs of fields with greater than four rows of tubules between neighboring vascular bundles were systematically obtained with the vascular bundles at the periphery of micrographs. We evaluated an average of 9 to 10 (range, 5–18) photomicrographs per rat. If photos from the first section contained less than 200 TALs, additional sections were cut from separate tissue blocks, stained, and photographed. These color photomicrographs of double or triple stained sections were then analyzed using the following criteria. TALs adjacent to vascular bundles were defined as belonging to long-looped nephrons. TALs separated by at least one row of tubules from vascular bundles were defined as belonging to short-looped nephrons. These latter TALs were subdivided into two zones according to proximity to vascular bundles. Intermediate zone TALs were defined as those separated from vascular bundles by only one row of tubules, whereas those in the zone more distal from vascular bundles were separated from vascular bundles by at least two rows of tubules. The population of SL TALs in the zone more distal from vascular bundles was used for comparison of the frequency of luminal deposits in SL TALs to that in LL TALs. These TALs of SL nephrons represent a relatively pure population, because they are physically separated from LL TALs by a buffer zone of a single row of TALs. The number of TALs and the number of TALs with luminal deposits in each zone were recorded. The number of TALs evaluated per rat in sections perpendicular to medullary rays was 512 ± 54 in SHRs, 480 ± 55 in aging rats, 493 ± 28 in ADR rats, and 234 ± 45 in NX rats. Luminal deposits comparable to basal deposits in size and intensity were defined as 1+, whereas scores of 2+ and 3+ identified larger and more intense deposits.

Light microscopy studies were performed using portions of renal tissue fixed in neutral buffered formalin, embedded in glycolmethacrylate (GMA), sectioned at 2 μm with a Sorvall JB4 microtome (Dupont, Wilmington, Delaware), and stained with periodic acid-Schiff (PAS) and hematoxylin (Ishidate et al, 1983). The cortex was divided into three equal zones—deep, middle, and superficial—and glomeruli within the deep and superficial zones were examined microscopically under high power.

The size of glomeruli was assessed morphometrically in deep and superficial zones of cortex on a single section as previously described (Ikoma et al, 1990). The planar area of each glomerular capillary tuft within these areas was determined using a computerized planimeter (Micro-plan II, Monsanto Corporation, Natick, Massachusetts). The values of these planar areas for each of the zones were averaged on each specimen to obtain mean superficial and deep glomerular areas for each rat.

A semiquantitative score (sclerosis index) was determined to evaluate the degree of glomerular sclerosis (Raij et al, 1984). In this scoring system, segmental sclerosis is defined by the presence of areas of collapse of capillary lumina, adhesions of glomerular tuft to Bowman's capsule, and/or hyalinosis. Severity of sclerosis was graded from 0 to 4+ for each glomerulus using the same sections used for morphometric assessments. Accordingly, a 1+ lesion represented involvement of up to 25% of a glomerulus, whereas 4+ represented sclerosis of 75% to 100% of a glomerulus. The sclerosis index for each zone was then calculated by averaging the scores for all glomeruli present in the superficial and deep zones.

Statistical analysis was performed using the Statworks software program for the Apple Macintosh. Comparisons of data from individual kidneys were made using the paired *t* test and comparisons between groups were made using the unpaired *t* test. Correlations were examined by simple linear regression with two-tailed analysis of variance and by the Spearman's rank coefficient test. Data are expressed as means $\pm$ standard error (SEM). For single comparisons, p values < 0.05 have been adopted as significant.

Acknowledgements

Dr. Fogo is an Established Investigator of the American Heart Association. Dr. Delaney was supported by a research fellowship of the National Kidney Foundation. Ms. Tanya Clark provided technical assistance. Preliminary reports of portions of these studies have been presented at annual meetings of the American Society of Nephrology.

References

Allison ME, Wilson CB, and Gottschalk CW (1974). Pathophysiology of experimental glomerulonephritis in rats. *J Clin Invest* 53:1402–1423.

Bankir L and de Rouffignac C (1985). Urinary concentrating ability: Insights from comparative anatomy. *Am J Physiol*. 249:R643-R666.

Bolton WK, Benton FR, Maclay JG, and Sturgill BC (1976). Spontaneous glomerular sclerosis in aging Sprague-Dawley rats. *Am J Pathol* 85:277–302.

Bouby N, Trinh-Trang-Tan MM, Laouari DK, Kleinknecht C, Grunfeld JP, Kriz W, and Bankir L (1988). Role of the urinary concentrating process in the renal effects of high protein intake. *Kidney Int* 34:4–12.

Couser WG and Stilmant MM (1975). Mesangial lesions and focal glomerular sclerosis in the aging rat. *Lab Invest* 33:491–501.

Eddy AA (1994). Experimental insights into the tubulointerstitial disease accompanying primary glomerular lesions. *J Am Soc Nephrol* 5:1273–1287.

Elema JD and Arends A (1975). Focal and segmental glomerular hyalinosis and sclerosis in the rat. *Lab Invest* 33:554–561.

Feld LG, VanLiew JB, Galaske RG, and Boylan, JW (1977). Selectivity of renal injury and proteinuria in the spontaneously hypertensive rat. *Kidney Int* 12:332–343.

Fogo A, Yoshida Y, Glick AD, Homma T, and Ichikawa, I (1988). Serial micropuncture analysis of glomerular function in two rat models of glomerular sclerosis. *J Clin Invest* 82:322–330.

Fogo A and Ichikawa, I (1989). Evidence for the central role of glomerular growth promoters in the development of sclerosis. *Semin Nephrol* 9:329–342.

Friedman J, Hoyer JR, and Seiler MW (1982). Formation and clearance of tubulointerstitial immune complexes in kidneys of rats immunized with heterologous antisera to Tamm-Horsfall protein. *Kidney Int* 21:575–582.

Hoyer JR, Resnick JS, Michael AF, and Vernier RL (1974). Ontogeny of Tamm-Horsfall urinary glycoprotein. *Lab Invest* 30:757–761.

Hoyer JR, Bergstein JM, Michael AF, and Hoyer LW (1978). Immunofluorescent localization of Factor VIII related antigen and fibrinogen in hyperacute xenograft rejection and in the Shwartzman reaction in the rat. *Clin Immunol Immunopathol* 9:454–463.

Hoyer JR (1980). Tubulointerstitial immune complex nephritis in rats immunized with Tamm-Horsfall protein. *Kidney Int* 17:284–292.

Ichikawa I, Hoyer JR, Seiler MW, and Brenner BM (1982). Mechanisms of glomerulotubular balance in the setting of heterogeneous glomerular injury: Preservation of a close functional linkage between individual nephrons and surrounding microvasculature. *J Clin Invest* 69:185–198.

Ikoma M, Yoshioka T, Ichikawa I, and Fogo A (1990). Mechanism of the unique susceptibility of deep cortical glomeruli of maturing kidneys to severe focal glomerular sclerosis. *Pediatr Res* 28:270–276.

Ishidate T, Hoyer JR, and Seiler MW (1983). Influence of altered glomerular permeability on renal tubular immune complex formation and clearance. *Lab Invest* 49:582–588.

Ishidate T, Hebert D, Seiler MW, and Hoyer JR (1992). Immunomorphometric studies of proteinuria in individual nephrons of rats. *Lab Invest* 67:369–378.

Ishidate T, Ward HJ, and Hoyer JR (1990). Quantitative studies of tubular immune complex formation and clearance in normal rats and rats with increased glomerular permeability. *Kidney Int* 38:1075–1084.

Kees-Folt D, Sadow JL, and Schreiner GF (1994). Tubular catabolism of albumin is associated with the release of an inflammatory lipid. *Kidney Int* 45:1697–1709.

Kriz W, Schnermann J, and Koepsell H (1972). The position of short and long loops of Henle in the rat kidney. *Z Anat* Entwicklungsgesch 138:301–319.

Lemley KV and Kriz W (1987). Cycles and separations: The histotopography of the urinary concentrating process. *Kidney Int* 31:538–548.

Lewy JE and Pesce A (1973). Micropuncture study of albumin transfer in aminonucleoside nephrosis in the rat. *Pediatr Res* 7:553–559.

Oikawa T and Fogo A (1995). Mechanisms and significance of proteinuria. *Nephrology* 1:95–103.

Okuda S, Oochi N, Wakisaka M, Kanai H, Tamaki K, Nagase S, Onoyama K, and Fujishima M (1992). Albuminuria is not an aggravating factor in experimental focal glomerulosclerosis and hyalinosis. *J Lab Clin Med* 119:245–253.

Raij L, Azar S, and Keane W (1984). Mesangial immune injury, hypertension, and progressive glomerular damage in Dahl rats. *Kidney Int* 26:137–143.

Ruggenenti P, Perna A, Mosconi L, Pisoni R, and Remuzzi G (1998). Urinary protein excretion rate is the best independent predictor of ESRF in non-diabetic proteinuric chronic nephropathies. "Gruppo Italiano di Studi Epidemiologici in Nefrologia" (GISEN). *Kidney Int* 53:1209–1216.

Tanaka R, Kon V, Yoshioka T, Ichikawa I, and Fogo A (1994). Angiotensin converting enzyme inhibitor modulates glomerular function and structure by distinct mechanisms. *Kidney Int* 45:537–543.

Wehrmann M and Bohle A (1998). The long-term prognosis of benign nephrosclerosis accompanied by focal glomerulosclerosis and renal cortical interstitial fibrosis, designated so-called decompensated benign nephrosclerosis by Fahr, Bohle and Ratscheck. *Pathol Res Pract* 194:571–576.

Yoshioka T, Shiraga H, Yoshida Y, Fogo A, Glick AD, Rennke HG, Deen WM, Hoyer JR, and Ichikawa I (1988). "Intact Nephrons" as the primary origin of proteinuria in chronic renal disease: A study in the rat model of subtotal nephrectomy. *J Clin Invest* 82:1614–1623.